©IEEE, 2021. This is the authors' version of the work. Personal use of this material is permitted. However, permission to reprint/republish this material for advertising or promotional purpose or for creating new collective works for resale or redistribution to servers or lists, or to reuse any copyrighted component of this work must be obtained from the IEEE.
The definite version is published in Proc. IEEE ACSOS, Washington, DC, US, 2021.

Stochastic Switching of Power Levels can Accelerate Self-Organized Synchronization in Wireless Networks with Interference

Jorge F. Schmidt[1,2], Udo Schilcher[1], Arke Vogell[1], and Christian Bettstetter[1]
[1] University of Klagenfurt, Institute of Networked and Embedded Systems, Austria
[2] Lakeside Labs GmbH, Klagenfurt, Austria
email: jorge.schmidt@aau.at

***Abstract*—Studies on wireless network synchronization based on the theory of coupled oscillators largely ignore the interference caused by the in-band synchronization signals exchanged between nodes. We show that such interference can play a key role and gain two insights: First, increasing the node transmission power does not necessarily lead to faster synchronization. Second, synchronization can be accelerated by randomly switching between two power levels while maintaining the overall average power consumption. This approach temporarily boosts the network connectivity with negligible impact on the average interference. The special case with one of the power levels being zero links our approach to the known concept of stochastic coupling used in convergence proofs. In summary, our work suggests that a randomization of the coupling — e.g., using fewer but stronger synchronization signals — can have benefits for self-organizing synchronization in networks with interference.**

***Index Terms*—Pulse coupled oscillators, synchronization, self-organization, randomization, interference, stochastic geometry, IoT.**

1. Introduction

Wirelessly networked systems can be synchronized in time in a self-organizing manner using ideas from the theory of pulse-coupled oscillators (PCO) [1]. Attaining global synchronization in a decentralized manner is attractive for IoT applications: thousands of nodes deployed over a large area can be synchronized without any infrastructure [2], [3], [4], [5]. Extensive literature on PCO-like wireless synchronization covers adaptions to the theory (see [6], [7], [8], [9], [10], [11]), performance studies (see [12], [13]), and prototypical implementations (see [14], [15], [16], [17]).

Despite these advances, an important effect has largely been ignored so far: the mutual radio interference occurring when nodes broadcast synchronization information. The basic finding of this paper is that interference can fundamentally affect the synchronization performance. Interference may occur since most wireless systems use synchronization words embedded into messages rather than infinitely short pulses (assumed in PCO theory) to exchange states between nodes. The synchronization messages have to be decoded to distinguish them from other message types. This decoding process may fail if two or more messages overlap in time.

The role of interference is analyzed using a standard network model with nodes distributed as a Poisson point process and a fading channel [18], [19]. We highlight the effects of interference on the network connectivity and gain insights on the parameters to adjust in order to reduce the synchronization time. We start with a baseline scheme in which each node sends its synchronization messages at the end of each clock cycle with a baseline transmission power p or an increased power $p_{\text{high}} > p$. We find that a mere increase of the average transmission power does not necessarily accelerate synchronization due to the negative impact of interference.

Next, we propose and analyze an energy-neutral scheme that achieves faster synchronization than the baseline scheme in an interference scenario without increasing the average power consumption. The scheme randomly switches between two power levels: nodes transmit synchronization messages either with power p_{high} with probability μ or with power p_{low} with probability $1-\mu$. The decision of a node is independent from the decisions of other nodes and previous clock cycles. To achieve energy neutrality, we demand $p = \mu p_{\text{high}} + (1-\mu)p_{\text{low}}$. Of particular interest is the extreme case with $p_{\text{low}} = 0$. It is conceptually linked to the "stochastic interactions" approach [20], in which a node that is supposed to send a synchronization pulse does not always send it, but only with some probability smaller than one. In essence, we show that a randomization of the coupling network — caused, for example, by fewer but more powerful synchronization messages — results in faster synchronization in many scenarios.

The paper is organized as follows. Section 2 reviews PCO synchronization, introduces the network model, and motivates our approach. Section 3 analyzes the impact of interference on the network connectivity. Section 4 studies how transmission probability and power affect the synchronization time. Section 5 discusses the results. Section 6 summarizes the work related to ours. Section 7 concludes.

2. Models and Definitions

2.1. Synchronization

We consider a network modeled by a graph G consisting of nodes and links connecting the nodes. All nodes maintain identical oscillators. The current state of an oscillator is represented by a phase $\phi \in [0, 1]$. A freely running oscillator linearly increases its phase over time from $\phi = 0$ to 1 over a period of T time units (clock period). Whenever the phase reaches $\phi = 1$, it is reset to zero and a "fire event" occurs, which triggers the transmission of a synchronization message. Global phase synchronization results from the reaction to receiving synchronization messages over the links. Nodes connected to the firing node adjust their phase upon the reception of the message following a specific phase response function $f(\phi)$. We use the following piecewise linear mapping from $[0, 1]$ to $[0, 1]$:

$$f(\phi) = \begin{cases} (1-a)\,\phi & \text{for } \phi \leq 0.5 \\ (1-a)\,\phi + a & \text{for } \phi > 0.5\,. \end{cases} \quad (1)$$

The phase response parameter $a \in (0, 1)$ determines how strong a synchronization message modifies the phase of the receiving node [21], [22]. The design of the phase response function is an active research area (see, e.g., [13], [23]). We use the simple parametrization in (1), as it captures both inhibitory and excitatory coupling [24] with a single tuning parameter. Our results for this simple yet general parametrization provide insights on the synchronization performance that apply to more sophisticated phase responses.

A key performance metric is how fast synchrony is reached, measured in units of clock periods. The phase spread in the network quantifies how aligned the phases of the nodes are at a given time:

$$\epsilon(G) = 1 - \max_i(\delta_i) \text{ with } \delta_i = (\phi_{i-1} - \phi_i) \bmod 1, \quad (2)$$

where the nodes are numbered in i in ascending phase order. The *synchronization time* is defined as the number of clock cycles elapsed until ϵ reaches a small enough value.

2.2. Network model

Node placement. The nodes of G are randomly placed over an area $\|A\|$ in $\mathbb{R}^2$ with their positions sampled from a Poisson point process (PPP) Φ of intensity λ. For PPP, the expected number of nodes in the deployment is $N = \lambda\|A\|$.

Links and message exchange. Our channel model incorporates path loss, small-scale fading, and noise. A message s_i transmitted from node i with power p_i reaches a receiver j at a distance d_{ij} with average power $p_i d_{ij}^{-\alpha}$. The path loss exponent α of the environment has typical values $\alpha \in [2, 5]$. Variations around the average power due to multipath propagation are modeled by Rayleigh block fading. The fading power h_{ij} follows an exponential distribution of parameter 1 and is assumed to be constant over a message duration and independent for each transmission. The thermal noise $n(t)$ at the receiver is modeled as additive white Gaussian noise (AWGN) of variance σ^2. The power received at a node j at time t is

$$r_j(t) = \sum_{i \in \Phi/j} \mathbb{1}_j\, p_i\, d_{ij}^{-\alpha}\, h_{ij}(t)\, s_i(t) + n^2(t), \quad (3)$$

with the indicator function $\mathbb{1}_j$ being equal to one for messages reaching j at time t, and zero otherwise.

For linear receivers, the successful reception of a desired message is evaluated in terms of the signal-to-interference-and-noise (SINR) ratio and the receiver sensitivity γ_i. The SINR is the ratio between the power received from the desired message and that of the noise and interfering messages. If SINR $> \gamma_i$, the message is successfully decoded. The noise power is assumed to be small enough to be neglected, so we rely on the signal-to-interference ratio (SIR) only.

In a homogeneous system, all nodes use the same transmission power p and have the same receiver sensitivity γ.

Remark: The chosen combination of a stochastic spatial model (PPP) and fading channel model is often used to approximate real-world wireless networks — ranging from mobile to sensor networks and IoT systems, in different propagation conditions [25], [26], [27], [28]. It provides an analytical framework for the evaluation of large networks that can lead to insights that are much harder, if not impossible, to obtain from a network simulator.

2.3. Impact of Connectivity on Synchronization

Certain properties of a network graph have significant impact on the synchronization process in this network (see [29], [30]). For example, they govern the likelihood of convergence to synchrony and the synchronization time. We want to gain insights on how the network connectivity influences the synchronization in our network model.

Connectivity. The network graph G can be described by its adjacency matrix with elements $G_{ij} = 1$ if node i has a link to node j, and $G_{ij} = 0$ otherwise. The diagonal elements G_{ii} are zero per definition. In a homogeneous system, the graph is undirected, thus has a symmetric adjacency matrix with $G_{ij} = G_{ji}$. In this paper, we use the fraction of nonzero elements in the adjacency matrix excluding the diagonal to quantify what we call the *network connectivity* ρ.

Impact of connectivity on synchronization. We create a homogeneous random network with 30 nodes on average and assume links with pathloss but without fading. All results are the average of the synchronization times from 1000 realizations of random network deployments with nodes initialized with a uniformly distributed random phase between zero and one. Figure 1 (a) shows the empirical likelihood of convergence to synchrony as a function of connectivity ρ and phase response parameter a. In most network realizations, global synchrony is achieved for $\rho > 0.65$ and $0.35 < a < 0.55$, so we focus on these values in

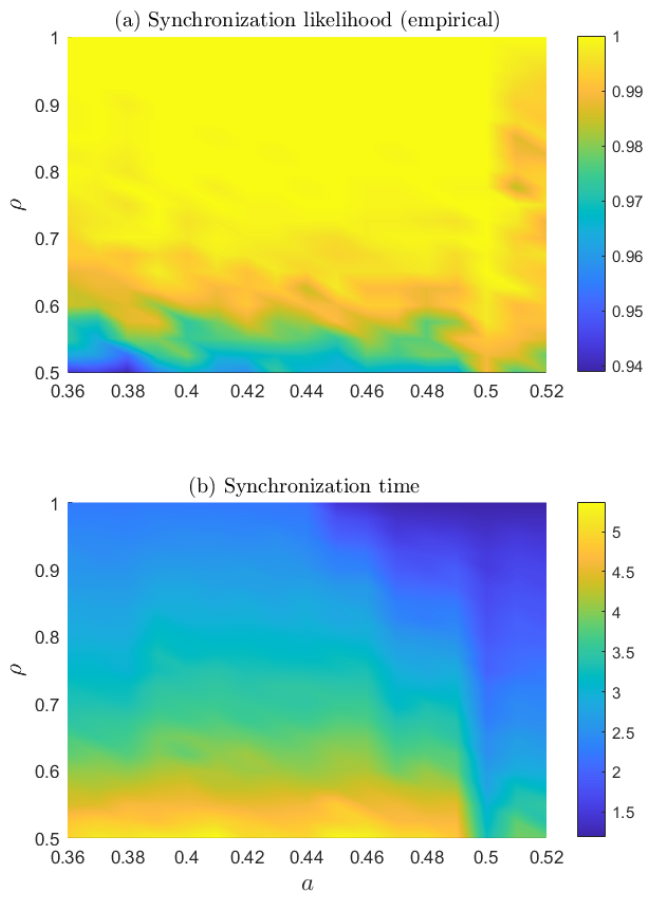

Figure 1. Synchronization convergence and speed in a homogeneous oscillator network as a function of the network connectivity ρ and the phase response parameter a for the given network model. When evaluating different node densities, the deployment area A is adjusted to keep the average number of nodes N constant.

this paper. Figure 1 (b) shows the synchronization time resulting for some (ρ, a)-pairs, which illustrates that a proper parameter choice can speed up the synchronization. For the phase response parameter, the fastest synchronization is achieved for $a \approx 0.5$. For the connectivity, the synchronization time decreases monotonically with increasing ρ, showing a comparatively low reduction as ρ approaches one; this monotonic behavior indicates that a better-connected network converges faster [31].

Based on these insights, we take the approach to speed up synchronization by modifying the network connectivity, and we perform such modification in a stochastic manner. The phase response parameter will remain fixed at $a = 0.5$. We do not investigate further its adjustment, as it is specific to the phase response function. Our goal is to gain insights on a general mechanism applicable to different phase response functions.

3. Connectivity and Interference

The role of interference should be considered for adapting PCO synchronization to wireless networks. But research on PCOs focuses on canonical network topologies and random on-off connection graphs that fail to capture fundamental interference features.

3.1. Interference-free impulse messages

In the theory of PCOs, the nodes exchange pulses (infinitely short messages without any data content) to inform each other about fire events. This ideal modeling approach can be employed in wireless systems if messages are short enough so that messages from different senders never overlap at the receiver, yielding an interference-free scenario.

In the absence of noise and interference, a message is successfully decoded if its received power r is above a threshold $\tilde{\gamma}$, which we denote with the same symbol γ of the receiver sensitivity, to simplify the notation. The success probability is thus obtained as

$$\begin{aligned} \mathrm{P_s} &= \Pr\{p\, h(t)\, d^{-\alpha} > \gamma\} = 1 - \Pr\left\{h(t) \leq \frac{d^{\alpha}\gamma}{p}\right\} \\ &= \exp\left(-\frac{d^{\alpha}\gamma}{p}\right), \end{aligned} \tag{4}$$

where the last line results from taking the expected value over the fading power (which is exponentially distributed with unit mean). The maximum distance for messages to be received is

$$d = \left(-\frac{p \ln \mathrm{P_s}}{\gamma}\right)^{\frac{1}{\alpha}}. \tag{5}$$

An estimate for the network connectivity ρ is the ratio between the circular area delimited by d and the area A:

$$\rho = \frac{\pi}{A}\left(-\frac{p \ln \mathrm{P_s}}{\gamma}\right)^{\frac{2}{\alpha}}. \tag{6}$$

Observe that the connectivity scales with $p^{2/\alpha}$. This implies that an increase in ρ requires an increase in power p, which turns higher for harsher propagation environments (high α).

3.2. Interference from overlapping messages

If messages cannot be modeled as pulses, as is the case in many practical systems, it is possible to have many terms in the sum from (3) at any time t. The communication range is shorter than with pulses, as the transmission of synchronization messages from different nodes overlap the desired synchronization message, thus degrading the SIR. The success probability becomes

$$\mathrm{P_s} = \Pr\{\mathrm{SIR(t)} > \gamma\} = \mathbb{E}_{h,\Phi}\left\{\Pr\left\{\frac{p\, d^{-\alpha}\, h(t)}{I(t)} > \gamma\right\}\right\}, \tag{7}$$

where $I(t) = \sum_{i \in \Phi \backslash 0} \eta p_i d_i^{-\alpha} h_i(t)$, with $\Phi \backslash 0$ indicates that the transmitter of the desired message is excluded. The index

of the desired transmitter in (7) is dropped, since, for a PPP, a node located at the origin reflects the typical link behavior. Coefficient η in the expression for $I(t)$ models the probability that a node is transmitting at time t. This coefficient increases to one as the PCOs evolve to synchrony, where all fire events occur simultaneously.

If all nodes use the same transmission power $p_i = p$, the SIR becomes

$$\mathrm{SIR}(t) = \frac{d^{-\alpha} h(t)}{\sum_{i \in \Phi \setminus 0} \eta d_i^{-\alpha} h_i(t)}. \tag{8}$$

The success rate for the typical link is evaluated from (8) as [19]

$$\mathrm{P_s} = \exp\left(-\pi\lambda\gamma^{2/\alpha}\eta d^2 \Gamma\left(1+\frac{2}{\alpha}\right)\Gamma\left(1-\frac{2}{\alpha}\right)\right), \tag{9}$$

with the Gamma function $\Gamma(\cdot)$. Analogously to the interference-free scenario, the mean communication range d_I is derived from (9) as

$$d_I = \left(-\frac{\ln(\mathrm{P_s})}{\pi\lambda\gamma^{2/\alpha}\eta\Gamma\left(1+\frac{2}{\alpha}\right)\Gamma\left(1-\frac{2}{\alpha}\right)}\right)^{\frac{1}{2}}, \tag{10}$$

and the connectivity results in

$$\rho_I = -\frac{\ln(\mathrm{P_s})}{A\lambda\gamma^{2/\alpha}\eta\Gamma\left(1+\frac{2}{\alpha}\right)\Gamma\left(1-\frac{2}{\alpha}\right)}. \tag{11}$$

Remark: When the algorithm starts, each node has a random phase, uniformly distributed in $[0, 1]$. With time normalized to the length of a synchronization message (such that T messages span a clock period), the natural firing frequency $\bar{\eta}$ of a node is $1/T$. This frequency gives the η used to evaluate the initial ρ of the network. As the algorithm progresses and the nodes' phases align, reception only occurs at fire events leading to a η-value tending to one.

3.3. Impact of interference on connectivity

Without interference, the synchronization progression does not change the connectivity of the network. With interference, however, parameter η in (8) degrades the SIR as the phases progress towards alignment, lowering the probability of successful reception of the synchronization messages. We assess the impact of this phenomenon on synchronization performance and compare it to a scenario without interference. For a fair comparison, we choose the network parameters in a way that the connectivity is the same for both scenarios when the algorithm starts. The values of $\mathrm{P_s}$ and γ remain fixed.

The expressions in (6) and (11) show that the two scenarios have different design parameters to tune the connectivity: In the interference-free scenario, the parameter to tune ρ is p. In the interference scenario, λ is adjusted in (11), such that $\rho = \rho_\mathrm{I}$. Adjusting λ is not practical in real implementations but enables comparison of the two scenarios. The practical tuning of ρ_I is discussed below.

Figure 2 gives some operating points, in which the connectivity is the same in both scenarios. These are given by the λ-values that intersect the connectivity traces for the corresponding γ. The value of p is read from the horizontal axis at the intersection. Without interference, a simple adjustment of p can meet any ρ for a given γ. In contrast, ρ_I is independent of p as an increase in p affects the desired signal and interference in the same way. If interference exists, a higher ρ is only obtained for low density.

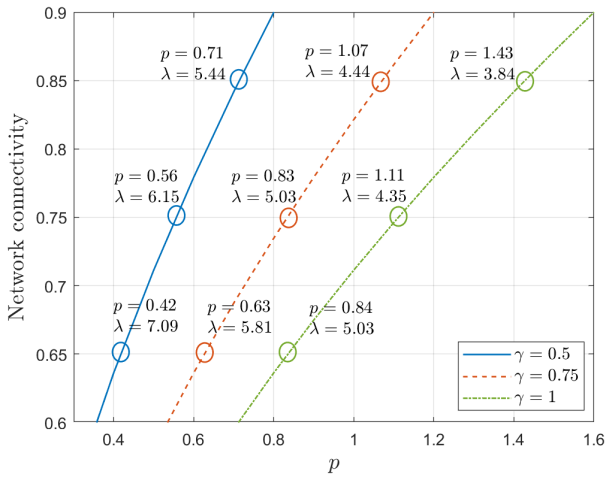

Figure 2. Pairs (p, λ) that reach $\rho = \rho_\mathrm{I}$ for connectivity targets of 0.65, 0.75, and 0.85. Each trace corresponds to a different γ. Results correspond to $\mathrm{P_s} = 0.95$, $\eta = 0.01$, $\alpha = 4$, and $p_i = p$ for all i.

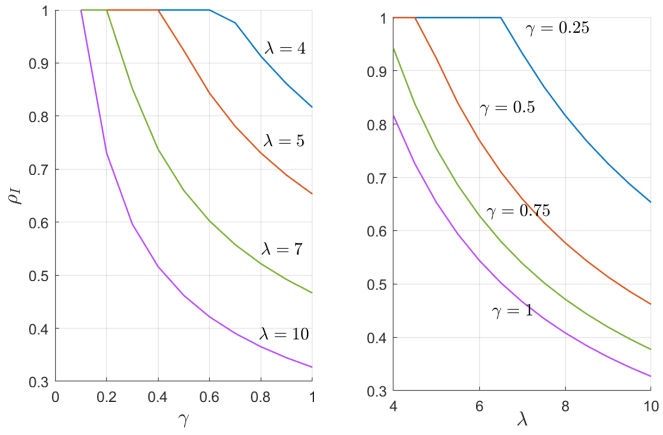

Figure 3. Practical adjustment of ρ_I. The left plot shows how γ can be adjusted to get different ρ_I targets depending on the network density λ. The right plot clarifies how the choice of γ limits the achievable ρ_I for a given network density λ. Settings are $\mathrm{P_s} = 0.95$, $\eta = 0.01$, $\alpha = 4$, and $p_i = p$ for all i.

3.4. Adjusting ρ_I in a practical implementation

The density is a parameter outside of the design scope. A practical design for an interference scenario tunes the receiver sensitivity to reach a ρ_I-value that leads to convergence, as shown in the left part of Figure 3 for $\mathrm{P_s} = 0.95$

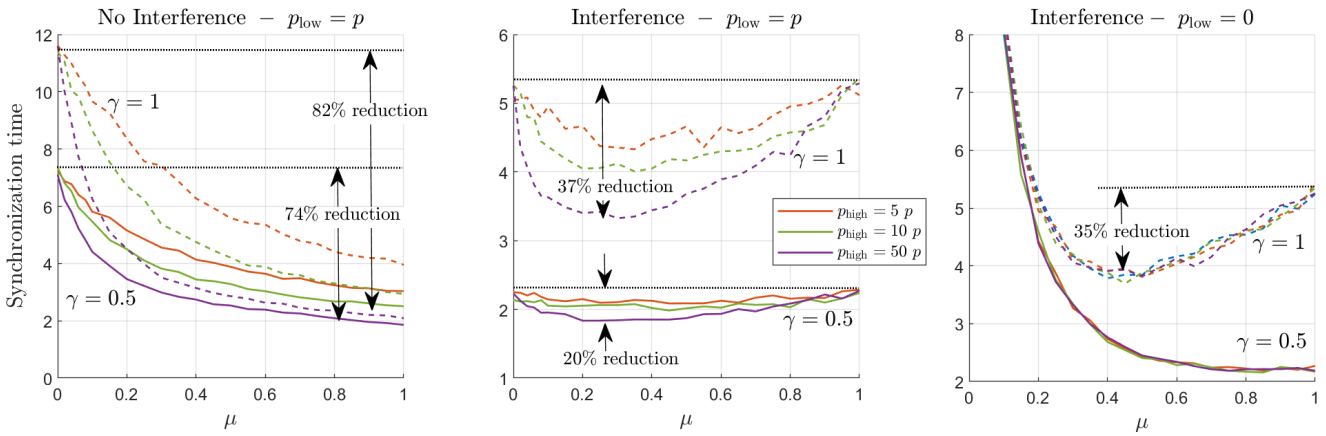

Figure 4. Synchronization time with stochastic connectivity boosts. The left plot shows the results for the interference-free scenario, the center plot for the interference scenario, and the right plot for the interference scenario with $p_{\text{low}} = 0$ instead of p. Values correspond to $\text{P}_\text{s} = 0.95$, $\eta = 0.01$, and $\alpha = 4$.

and some λ-values. The right part of the figure highlights the limitation of adjusting γ. Lower γ-values imply higher ρ_I, but the density limits how high ρ_I can become. For example, $\rho_\text{I} > 0.9$ cannot be reached for $\gamma = 0.25$ if $\lambda > 7.2$. Also, for low λ, a too small γ-value might be impossible due to hardware constraints. In that case, the success probability is relaxed.

4. Synchronization with Power Switching

4.1. Stochastic power boosts

Consider the *alternation* between two power levels p_{low} and p_{high}. The lower power level $p_{\text{low}} = p$ is chosen from Figure 2 to match a circled operating point (p, λ) that meets a target ρ. The higher power level p_{high} is used with probability μ at a fire event. The goal is to achieve a flexible trade-off between synchronization time and power consumption. This stochastic alternation is based on insights from the interference-free scenario. In the interference scenario, ρ changes as the algorithm progresses (because of the non-constant η). Specifically, we propose to set $p_{\text{high}} = kp$, with $k \in \mathbb{R}^+$. Upon a fire condition, the node decides to use p_{high} with probability μ (and p_{low} with probability $1 - \mu$), with μ selected to meet a desired power consumption. This mechanism leads to an improved connectivity $\bar{\rho}$ given by

$$\bar{\rho} = \mu\rho_{\text{high}} + (1 - \mu)\rho, \tag{12}$$

where ρ_{high} is obtained by replacing p_{high} in (6):

$$\rho_{\text{high}} = \frac{\pi}{A}\left(-\frac{p_{\text{high}} \ln(\text{P}_\text{s})}{\gamma}\right)^{\frac{2}{\alpha}} = k^{\frac{2}{\alpha}}\rho. \tag{13}$$

Combining (12) and (13) yields

$$\bar{\rho} = \rho\left(\mu(k^{\frac{2}{\alpha}} - 1) + 1\right) > \rho \qquad \text{for} \quad k > 1. \tag{14}$$

Figure 4 shows the resulting synchronization time in three interference scenarios. In all plots, $\mu = 0$ corresponds to the case when the high power is never used, and $\mu = 1$ means that all messages are transmitted with high power. Our first observation is that the synchronization time monotonically decreases with increasing μ (i.e., the average transmission power is higher) when no interference exist. The higher the value of p_{high}, the faster the network synchronizes. However, the relative gain decreases for higher p multiples, as indicated by the fact that the traces for $p_{\text{high}} = 10p$ and $50p$ are close together.

If interference occurs, higher p_{high}-values also achieve faster synchronization, but the behavior in terms of μ is fundamentally different. A mere increase in the transmission power ($\mu = 1$) does not lead to a synchronization faster than the baseline ($\mu = 0$). The reason is: if a single power level is used, the connectivity is independent of the power value (recall (11)). In contrast, the stochastic power boosts ($\mu < 1$) lead to gains, as the high-power transmissions temporally increase the connectivity. Traces for different p_{high} and γ exhibit the same qualitative shape, with a minimum for relatively low μ. Table 1 summarizes the attained gains.

TABLE 1. SYNCHRONIZATION TIME GAINS STOCHASTIC POWER BOOSTS

INTERFERENCE-FREE SCENARIO ($p_{\text{low}} = p$, $p_{\text{high}} = kp$)

	$\gamma = 0.5$			$\gamma = 1$		
k	5	10	50	5	10	50
Time reduction	59%	66%	74%	65%	74%	82%

INTERFERENCE SCENARIO ($p_{\text{low}} = p$, $p_{\text{high}} = kp$)

	$\gamma = 0.5$			$\gamma = 1$		
k	5	10	50	5	10	50
Optimal μ	0.40	0.30	0.25	0.35	0.3	0.25
Time reduction	8%	17%	20%	17%	24%	37%

Remark: The derived ρ_I is independent of p. However, stochastic connectivity boosts ($\mu < 1$) deviate from the assumptions that led to (11), since not all nodes use the same p all the time. The rightmost plot in Figure 4 better illustrates this point by plotting the achieved synchronization

times when $p_{\text{low}} = 0$ instead of p. In that case, independent of μ, all synchronization messages have power p_{high}. An optimal μ still exists for each γ, but traces for all p_{high} overlap as a single power level in agreement with (11).

4.2. Energy-neutral stochastic power switching

Stochastic power boosts can lead to faster synchronization, but these gains come at the expense of an increased overall power consumption. In many applications where PCO synchronization is of interest, nodes are battery-operated, and a permanently high transmission power is undesirable. Increasing ρ via an increase of transmission power significantly shortens the battery lifetime. We next adapt the scheme for the case in which the power budget at the nodes is fixed to obtain a power-fair comparison. In this case, p_{low} and p_{high} need to satisfy

$$p = \mu p_{\text{high}} + (1-\mu) p_{\text{low}}. \tag{15}$$

Again, we introduce a tuning parameter k to control how the two power levels relate to each other and set $p_{\text{high}} = k\, p_{\text{low}}$, which inserted in (15) leads to

$$p_{\text{low}} = \frac{p}{\mu(k-1)+1}, \qquad p_{\text{high}} = \frac{kp}{\mu(k-1)+1}, \tag{16}$$

such that the average power consumption is unchanged and the average connectivity remains improved:

$$\bar{\rho} = p\left(\frac{1+\mu(k-1)}{\mu(k-1)}\right) > p. \tag{17}$$

Figure 5 shows the results for the scheme defined by (16). The baseline corresponds to $\mu = 0$ and 1, where a single power p is used. The upper plot shows that for the interference-free scenario the alternation between p_{low} and p_{high} is incapable of reducing the synchronization time. Moreover, for $p_{\text{high}} \gg p_{\text{low}}$, performance is significantly degraded as μ decreases. For low k, we have $p_{\text{high}} \to p_{\text{low}} \to p$, and the baseline is attained. In contrast, when subject to interference, the stochastic alternation between powers always outperforms the baseline. Traces follow a trend similar to the case without power restrictions, and show comparable gains. The effect of k is opposite to the one observed for the interference-free scenario. Best results are obtained for $p_{\text{high}} \gg p_{\text{low}}$, suggesting that a single power level, setting $p_{\text{low}} = 0$ and $p_{\text{high}} = p/\mu$ is optimal.

The alternation between two power levels can be linked to the concept of stochastic coupling from [20]. That work studies how convergence to synchrony is affected if nodes reaching the firing condition send the synchronization message only sometimes rather than always. To be more specific, at each fire condition, a node transmits a synchronization message with a probability μ strictly smaller than 1. This condition is reached in the limit case in which $p_{\text{low}} = 0$ and only messages with power p_{high} are sent, with probability μ (see (15)). Transmitting only a fraction of the synchronization messages is enough to guarantee synchronization [20], and the synchronization speed decreases only slightly for

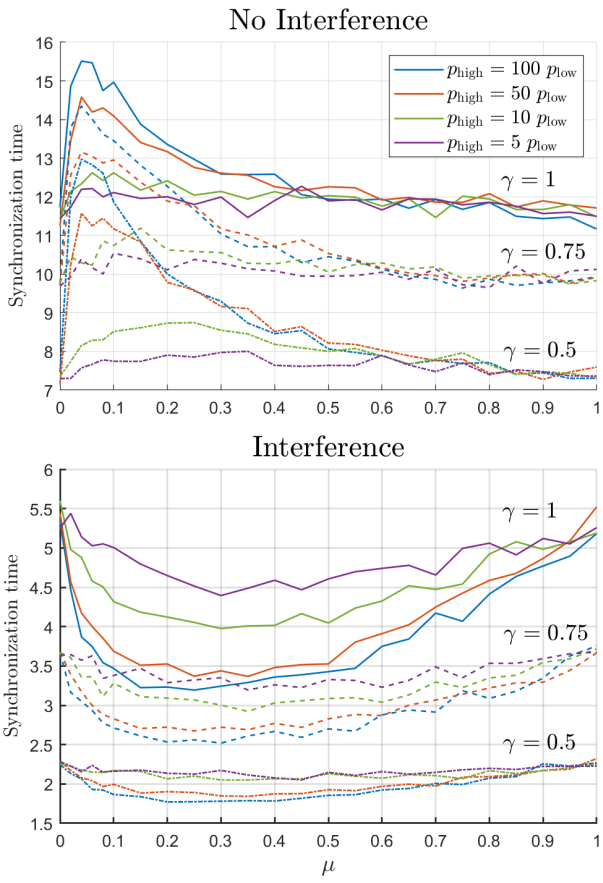

Figure 5. Synchronization time for stochastic power-constrained connectivity boosts. The top/bottom plot shows the results for the interference-free/interference scenarios, respectively. Values correspond to $P_s = 0.95$, $\eta = 0.01$, and $\alpha = 4$.

coupling probabilities down to about $1/2$ (top plot in Figure 6). Synchronization speed monotonically decreases for stochastic coupling where p_{high} is fixed and independent of μ. This happens because there is no connectivity increase (see (14) with $k = 1$) and fewer fire messages are sent. Our observation in Figure 5 suggests that it is possible to speed up the synchronization process by transmitting the synchronization messages less often but with higher power, constrained on the energy budget. To explore this idea, we adapt our design by setting $p_{\text{low}} = 0$ and $p_{\text{high}} = p/\mu$. We find that by adapting p_{high} to the value of μ, the mean connectivity $\bar{\rho}$ in (17) remains improved (bottom plot in Figure 6), in agreement with the behavior in Figure 5.

Figure 7 shows the synchronization time for the single power level scheme with a power constraint. Small μ-values lead to seldom transmissions of synchronization messages. In the limit $\mu = 0$, no messages are transmitted at all ($p_{\text{low}} = 0$), so the network does not synchronize. The baseline scenario corresponds to $\mu = 1$, where messages are always transmitted with power p. We observe the following: No improvements are obtained in the interference-free scenario, making this variant useless for that case. In contrast, is in-

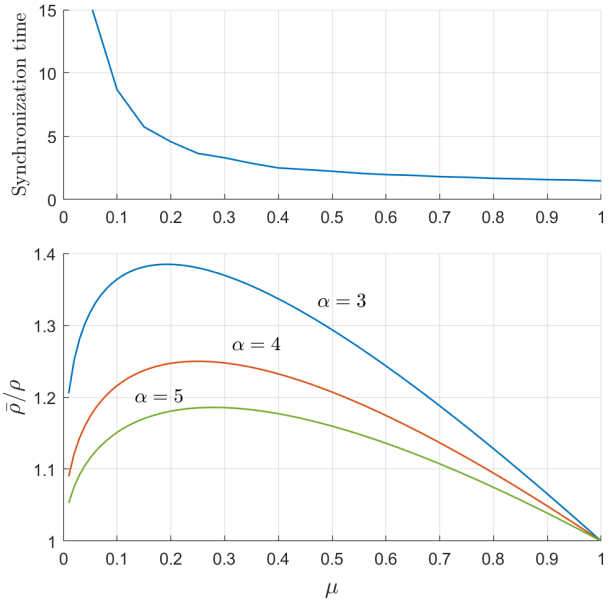

Figure 6. Relation between the stochastic coupling proposed in [20] and our power-constrained scheme with $p_{\text{low}} = 0$. The top plot shows the synchronization time for the stochastic coupling in [20]. The bottom plot shows the relative connectivity increase in terms of the probability of a high power transmission for our scheme. Traces correspond to different propagation conditions, through the path-loss exponent α.

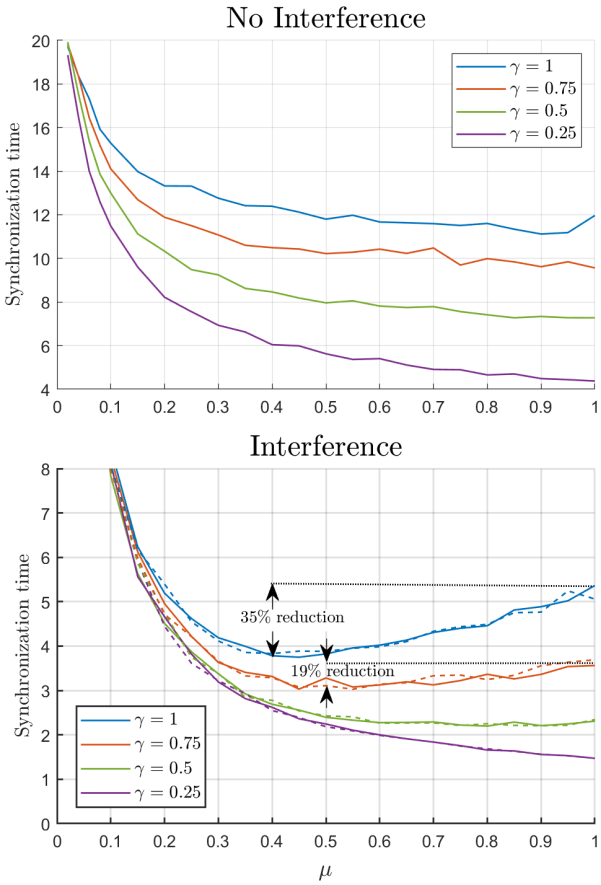

Figure 7. Synchronization time for stochastic power-constrained connectivity boosts and $p_{\text{low}} = 0$.The top/bottom plot shows the results for the interference-free/interference scenarios, respectively. Values correspond to $P_s = 0.95$, $\eta = 0.01$, and $\alpha = 4$.

terference occurs, improvements can indeed be achieved — at least for most γ-values tested. For $\gamma > 0.5$, there is always an improvement, with higher relative improvements for higher γ. For the interference scenario, results for $\rho = 0.85$ are also presented in dashed lines. These show that the synchronization time is not significantly improved for higher ρ.

5. Discussion and Outlook

If interference can be neglected, it is possible to speed up synchronization by increasing the transmission power. The intuition is that an higher power improves the connectivity so that synchronization messages reach farther. The largest gain is for a permanent power increase (i.e., $\mu = 1$), but most of the gain can be realized already for much lower values ($\mu < 0.4$), with up to 80 % faster synchronization. This acceleration comes with a significantly increased power consumption, which may not be practical for battery-powered devices. If the power budget is fixed, the performance changes drastically. No gain can be realized and the system reduces to stochastic coupling [20], where synchronization time only degrades for $\mu < 1$.

If interference occurs, the behavior is fundamentally different. A mere increase of the transmission power produces no benefit, as it scales outreach and interference in the same proportion. Nevertheless, with stochastic alternation between low-power and high-power messages, an optimum in the synchronization time exists (in the range from $\mu = 0.25$ to 0.5 in our model) for both constrained and unconstrained power budgets. Setting the low-power level to zero and using only the high-power level, synchronization can still be accelerated. This shows that the concept of stochastic coupling does not only guarantee convergence [20], it also reduces the synchronization time if power is concentrated over few strong synchronization messages.

Envisioned future research focuses on the interference scenario, where an initial next step would be to analyze the impact of other interference sources. These sources can be non-synchronization messages or interference from external systems. Both their analysis and possible mitigation of adverse effects are of interest. Another research direction concerns the design of local adaptation rules. The random node locations of practical deployments leads to some more connected or more isolated nodes. In groups of nodes that are in close proximity, very high-power levels, or a high μ, may not contribute to a global faster synchronization. Energy can be saved by adapting these parameters to teh local environment. Furthermore, rather isolated nodes may benefit from seldom higher power transmissions.

6. Related Work

The role of interference in PCO-based synchronization has not been investigated in depth so far. One reason for this lack of research could be the close relation of this synchronization approach with natural phenomena, where simultaneous reception of synchronization pulses actually strengthens the pulses and can turn beneficial to the synchronization process (denoted as absorption in [1]). Most research applying this synchronization concept to wireless networks continues to consider interference to be helpful or relies on interference being small enough to be disregarded (see [32], [33], [34]).

Some contributions assessing the impact of interfering synchronization messages include the experimental assessment in [35] and the numerical investigation in [15]. These contributions provide valuable insights into the impact of interference but lack an analytical framework to analyze further interference in different communication conditions. The framework provided in Section 3 provides a path towards such a more general analysis.

Other authors take a proactive approach to interference by embedding mechanisms in the synchronization algorithm to avoid it. They reduce the number of collisions between synchronization messages by adding a random delay to the fire events [14] and using of bursts of shorter messages [36]. These contributions provide mechanisms to minimize interference but do not model its network-wide effect, as done in the paper at hand.

Certainly, interference has been accounted for in non-PCO synchronization. Similar to our work, some papers propose a model for the interfering signals from which a synchronization sequence can be optimized [37], new synchronization algorithms can be built [38], and coordination strategies can be designed [39]. To the best of our knowledge, we are the first to propose an interference-aware design path for PCO synchronization.

7. Conclusions

We showed how the connectivity relates to the synchronization speed of a PCO scheme in a network model that approximates practical wireless deployments. We investigated how stochastic power boosts can accelerate synchronization and discussed design insights for interference-free and interference scenarios. Overall, it is shown that stochastic power alternation leads to faster synchronization in many scenarios and conditions. The fact that the interference scenario shows good performance for both the increased and fixed power setups is particularly interesting, as interference is a prevalent phenomena in wireless networks.

Acknowledgments

This work was partly funded by the Austrian Science Fund (FWF), grant "Self-organizing synchronization with stochastic coupling" (P30012) and by the Austrian Klima und Energiefonds under grant No. 881161 ("Condition and energy monitoring with innovative, ultra-reliable wireless sensor networks") in the 6. call of the energy research ("Energieforschung") program of the Austrian Research Promotion Agency (FFG).

References

[1] R. Mirollo and S. Strogatz, "Synchronization of pulse-coupled biological oscillators," *SIAM J. Appl. Math.*, vol. 50, pp. 1645–1662, 1990.

[2] R. Du, P. Santi, M. Xiao, A. V. Vasilakos, and C. Fischione, "The sensable city: A survey on the deployment and management for smart city monitoring," *IEEE Commun. Surveys Tuts.*, vol. 21, no. 2, Nov. 2018.

[3] E. Sisinni, A. Saifullah, S. Han, U. Jennehag, and M. Gidlund, "Industrial Internet of things: Challenges, opportunities, and directions," *IEEE Trans. Ind. Informat.*, vol. 14, no. 11, pp. 4724–4734, Nov 2018.

[4] V. K. L. Huang, Z. Pang, C. A. Chen, and K. F. Tsang, "New trends in the practical deployment of industrial wireless: From noncritical to critical use cases," *IEEE Ind. Electron. Mag.*, vol. 12, no. 2, pp. 50–58, Jun 2018.

[5] R. Du, L. Gkatzikis, C. Fischione, and M. Xiao, "On maximizing sensor network lifetime by energy balancing," *IEEE Trans. Control Netw. Syst.*, vol. 5, no. 3, pp. 1206–1218, Sep. 2018.

[6] R. Mathar and J. Mattfeldt, "Pulse-coupled decentral synchronization," *SIAM J. Appl. Math.*, vol. 56, no. 4, p. 1094–1106, Aug 1996.

[7] R. Holzer, H. Meer, and C. Bettstetter, "On autonomy and emergence in self-organizing systems," in *Int. Workshop on Self-Organizing Syst.*, 2008, pp. 157–169.

[8] R. Leidenfrost, W. Elmenreich, and C. Bettstetter, "Fault-tolerant averaging for self-organizing synchronization in wireless ad-hoc networks," in *Int. Symp. on Wireless Commun. Syst.*, Sep 2010, pp. 721–725.

[9] Z. An, H. Zhu, X. Li, C. Xu, and Y. Xu, "Nonidentical linear pulse-coupled oscillators model with application to time synchronization in wireless sensor networks," *IEEE Trans. Ind. Electron.*, vol. 58, pp. 2205–2215, 2011.

[10] Y. Iori and H. Ishii, "A resilient synchronization protocol for pulse-coupled oscillators over robust networks," *American Control Conf.*, pp. 713–718, Jul 2020.

[11] Z. Wang and Y. Wang, "Global synchronization of pulse-coupled oscillator networks under byzantine attacks," *IEEE Trans. on Signal Proc.*, vol. 68, pp. 3158–3168, 2020.

[12] R. Pagliari and A. Scaglione, "Scalable network synchronization with pulse-coupled oscillators," *IEEE Trans. Mobile Computing*, vol. 10, pp. 392–405, 2011.

[13] Y. Wang and F. J. Doyle III, "Optimal phase response functions for fast pulse-coupled synchronization in wireless sensor networks," *IEEE Trans. Signal Proc.*, vol. 60, no. 10, pp. 5583–5588, 2012.

[14] G. Werner-Allen, G. Tewari, A. Patel, M. Welsh, and R. Nagpal, "Firefly-inspired sensor network synchronicity with realistic radio effects," in *ACM Proc. Int. Conf. on Embedded Networked Sensor Syst.*, 2005, p. 142–153.

[15] R. Gentz, A. Scaglione, L. Ferrari, and Y. Hong, "PulseSS: A microcontroller implementation of pulse-coupled scheduling and synchronization protocol for cluster-based wireless sensor networks," *IEEE World Forum on Internet of Things*, pp. 536–541, 2015.

[16] G. Brandner, U. Schilcher, and C. Bettstetter, "Firefly synchronization with phase rate equalization and its experimental analysis in wireless systems," *Comput. Networks*, vol. 97, pp. 74–87, 2016.

[17] W. Masood and J. F. Schmidt, "Realizing pulse-coupled oscillators synchronization on IEEE 802.15.4 wireless networks," in *ITG Int. Conf. on Syst. Commun. and Coding*, 2017.

[18] S. Chiu, D. Stoyan, W. Kendall, and J. Mecke, *Stochastic Geometry and Its Applications*. Wiley, 2013.

[19] M. Haenggi, *Stochastic Geometry for Wireless Networks*. Cambridge University Press, 2012.

[20] J. Klinglmayr, C. Kirst, C. Bettstetter, and M. Timme, "Guaranteeing global synchronization in networks with stochastic interactions," *New J. of Physics*, vol. 14, pp. 73 031–73 044, 2012.

[21] H. Daido, "Intrinsic fluctuations and a phase transition in a class of large populations of interacting oscillators," *J. of Stat. Phy.*, vol. 60, pp. 753–800, 1990.

[22] S. Strogatz, "From Kuramoto to Crawford: exploring the onset of synchronization in populations of coupled oscillators," *Physica D: Nonlinear Phenomena*, vol. 143, pp. 1–20, 2000.

[23] Y. Wang, F. Núñez, and F. J. Doyle, "Increasing sync rate of pulse-coupled oscillators via phase response function design: Theory and application to wireless networks," *IEEE Trans. Control Syst. Tech.*, vol. 21, no. 4, pp. 1455–1462, 2013.

[24] C. Vreeswijk, L. Abbott, and B. Ermentrout, "When inhibition not excitation synchronizes neural firing," *J. of Computational Neuroscience*, vol. 1, pp. 313–321, 2004.

[25] W. Lu and M. Renzo, "Stochastic geometry modeling of cellular networks: Analysis, simulation and experimental validation," in *ACM Int. Conf. on Modeling, Anal. and Sim. of Wireless and Mobile Syst.*, 2015, p. 179–188.

[26] U. Schilcher, J. Schmidt, and C. Bettstetter, "On interference dynamics in matérn networks," *IEEE Trans. Mobile Computing*, vol. 19, pp. 1677–1688, 2020.

[27] J. Schmidt, U. Schilcher, M. K. Atiq, and C. Bettstetter, "Interference prediction in wireless networks: Stochastic geometry meets recursive filtering," *IEEE Trans. Vehicular Tech.*, vol. 70, pp. 2783–2793, 2021.

[28] Y. Hmamouche, M. Benjillali, S. Saoudi, H. Yanikomeroglu, and M. Di Renzo, "New trends in stochastic geometry for wireless networks: A tutorial and survey," *Proceedings of the IEEE*, Mar. 2021.

[29] M. Rohden, A. Sorge, D. Witthaut, and M. Timme, "Impact of network topology on synchrony of oscillatory power grids," *Chaos*, vol. 24, p. 013123, 2014.

[30] A. Townsend, M. Stillman, and S. H. Strogatz, "Dense networks that do not synchronize and sparse ones that do," *Chaos*, vol. 30, p. 083142, 2020.

[31] M. Timme, F. Wolf, and T. Geisel, "Topological speed limits to network synchronization," *Phys. Rev. Lett.*, vol. 92, p. 074101, Feb 2004.

[32] Y.-W. Hong and A. Scaglione, "Time synchronization and reach-back communications with pulse-coupled oscillators for UWB wireless ad hoc networks," in *IEEE Conf. Ultra Wideband Syst. and Tech.*, 2003, pp. 190–194.

[33] D. Lucarelli and I.-J. Wang, "Decentralized synchronization protocols with nearest neighbor communication," in *ACM Int. Conf. on Embedded Networked Sensor Syst.*, 2004, p. 62–68.

[34] Y. Wei and D.-S. Kim, "A self-stabilized firefly synchronization method for the ISA100.11a network," in *IEEE Int. Conf. ICT Convergence*, 2013, pp. 881–886.

[35] G. Smart, N. Deligiannis, R. Surace, V. Loscri, G. Fortino, and Y. Andreopoulos, "Decentralized time-synchronized channel swapping for Ad Hoc wireless networks," *IEEE Trans. on Vehic. Tech.*, vol. 65, no. 10, pp. 8538–8553, 2016.

[36] S. Bush, "Low-energy sensor network time synchronization as an emergent property," in *IEEE Int. Conf. Computer Commun. and Networks*, 2005, pp. 93–98.

[37] X. Luo and G. B. Giannakis, "Raise your voice at a proper pace to synchronize in multiple Ad Hoc piconets," *IEEE Trans. on Signal Processing*, vol. 55, no. 1, pp. 267–278, 2007.

[38] P. Amin and O. Tirkkonen, "Network listening based synchronization techniques for femtocell systems," in *IEEE Int. Symp. Personal, Indoor and Mobile Radio Commun.*, 2011, pp. 1–5.

[39] P. Amin, V. P. K. Ganesan, and O. Tirkkonen, "Bridging interference barriers in self-organized synchronization," in *IEEE Int. Conf. Self-Adaptive and Self-Organizing Syst.*, 2012, pp. 109–118.